Pergamon

Mech. Mach. Theory Vol. 33, No. 1/2, pp. 7–20, 1998

Printed in Great Britain
PII: S0094-114X(97)00025-6
0094-114X/98 $19.00 + 0.00

WORKSPACES OF PLANAR PARALLEL MANIPULATORS

JEAN-PIERRE MERLET
INRIA Sophia-Antipolis, BP 93, 06902 Sophia-Antipolis Cedex, France

and

CLÉMENT M. GOSSELIN
Dép. de Génie Mécanique, Université Laval, Ste-Foy, Québec, Canada G1K 7P4

and

NICOLAS MOULY
INRIA Rhône-Alpes, 46 Av. Felix Viallet, 38062 Grenoble, France

(Received 27 November 1996)

Abstract—This paper presents geometrical algorithms for the determination of various workspaces of planar parallel manipulators. Workspaces are defined as regions which can be reached by a reference point C located on the mobile platform. First, the *constant orientation* workspace is determined. This workspace is defined as the region which can be reached by point C when the orientation of the moving platform is kept constant. Then, the *maximal* workspace, which is defined as the region which can be reached by point C with at least one orientation, is determined. The maximal workspace is also referred to as the *reachable* workspace. From the above regions, the *inclusive* workspace, i.e. the region which can be attained by point C with at least one orientation in a given range, can be obtained. Then, the *total orientation* workspace, i.e. the region which can be reached by point C with every orientation of the platform in a given range, is defined and determined. Finally, the *dextrous* workspace, which is defined as the region which can be reached by point C with any orientation of the platform, can be determined. Three types of planar parallel manipulators are briefly described and one of them is used to illustrate the algorithms. Each of the workspaces is determined here for this type of manipulator while the derivations for the other types of manipulators will be presented in another paper. The algorithms developed here are useful in the design and motion planning of planar parallel manipulators. © 1998 Elsevier Science Ltd

1. INTRODUCTION

Parallel manipulators have been proposed as mechanical architectures which can overcome the limitations of serial robots [1]. Several mechanical architectures of parallel mechanisms can be found in the literature (see for instance [1]). Parallel manipulators lead to complex kinematic equations and the determination of their workspace is a challenging problem. However, the solution of this problem is very important in the design and trajectory planning of the manipulators. Some researchers have addressed the problem of the determination of the workspace of parallel manipulators [2–5].

In this paper, the problem of the determination of the workspaces of planar three-degree-of-freedom parallel manipulators is addressed. Algorithms are proposed for the determination of the maximal workspace, a problem which has been elusive to previous analyses. Moreover, this leads to the definition and determination of the total orientation workspace.

Planar three-degree-of-freedom parallel manipulators are composed of three kinematic chains connecting a mobile platform to a fixed base. Different types of manipulators are obtained depending on the nature of these chains. The manipulator of particular interest in this study is referred to as the 3-RPR manipulator. In this manipulator, the mobile platform is connected to the base via three identical chains consisting of a revolute joint attached to the ground followed by an actuated prismatic joint which is connected to the platform by a revolute joint (Fig. 1). Only the prismatic joints are actuated. Henceforth, the center of the joint connecting the ith chain to

the ground will be denoted A_i and the center of the joint connecting the ith chain to the platform will be referred to as B_i. Other types of planar parallel manipulators are:

- the 3-RRR robot [1, 6, 7] in which the three kinematic chains connecting the platform to the base are composed of two links and three revolute joints. The joint attached to the ground is the only actuated joint in each of the chains.
- the 3-PRR robot in which each kinematic chain is constituted of a prismatic actuator fixed to the base and a link attached both to the actuator and the moving platform by revolute joints.

For these last two types of robots, the description of the workspaces can be derived from the study of the 3-RPR manipulator and will be presented in another paper.

A fixed reference frame is defined on the base and a moving reference frame is attached to the platform with its origin at a reference point C. The position of the moving platform is defined by the coordinates of point C in the fixed reference frame and its orientation is given by the angle θ between one axis of the fixed reference frame and the corresponding axis of the moving frame.

For the 3-RPR manipulator, the workspace limitations are due to the limitations of the prismatic actuators. The maximum and minimum length of the prismatic actuator of the jth chain are denoted $\rho^j_{\max}$, $\rho^j_{\min}$. These values will be referred to as *extreme values* of the joint coordinates. It is assumed here that this planar mechanism is designed in such a way that no mechanical interference can occur between the links.

Furthermore, an *annular region* is defined as the region which lies between two concentric circles with different radii. The circle with the largest radius will be referred to as the *external circle* and the smaller circle will be referred to as the *internal circle*. The internal circle may not exist.

The dimensions of the manipulators which are used in the examples are given in the Appendix. In what follows, the presentation of the various workspaces will focus on the 3-RPR manipulator. *It must be noted that the algorithms have been implemented and all the drawings presented in this paper are results from this program.* Finally it is also pointed out that Sections 2 and 6 of this paper recall some known results which are included here so that this work fully covers the computation of all the possible types of workspace.

2. CONSTANT ORIENTATION WORKSPACE

The *constant orientation workspace* is defined as the region which can be reached by the reference point C when the moving platform has a constant orientation. The algorithm for the determination of the boundary of this workspace is well known and has been described in [8] and [5]. The orientation of the platform of the manipulator is defined here as the angle between the x axis of the fixed frame and the line going from B_3 to B_1.

It is first observed that for any position of C on the boundary of the workspace, at least one of link length should be at one of its extreme values. Indeed, if this condition is not met, the

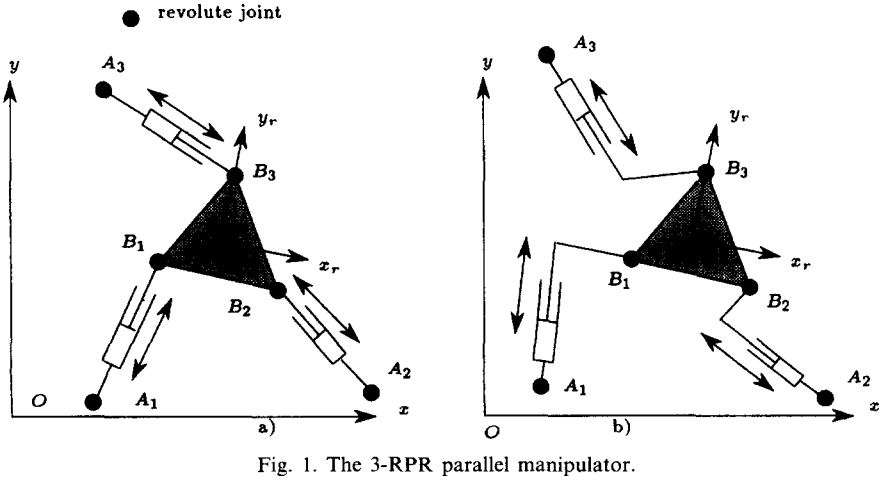

Fig. 1. The 3-RPR parallel manipulator.

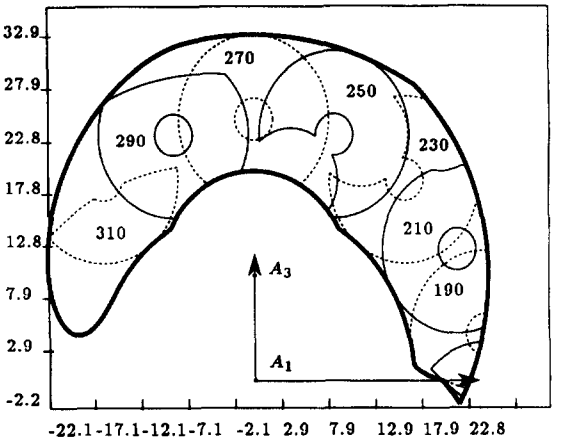

Fig. 2. Examples of constant orientation workspaces for manipulator 1 of the Appendix (in thin and dashed lines). The region within the thick line is the maximal workspace which will be presented in the next section. For this manipulator, the joint limits are $\rho_1 \in [8, 12]$, $\rho_2 \in [5, 15]$, $\rho_3 \in [10, 17]$.

platform may move in any direction and therefore C cannot be located on the boundary of the workspace. Now, the region which can be reached by a point B_i is considered. This region is an annular region ϵ_i whose external circle is centered at A_i with radius $\rho^j_{\max}$ and whose internal circle has the radius $\rho^j_{\min}$. In what follows, the external circle is denoted ϵ^e_i and the internal circle ϵ^i_i. Since the orientation is fixed, the vector $\mathbf{CB_i}$ is constant. Consequently, when B_i lies in the annular region ϵ_i, C also lies in an annular region ϵ_{ic} whose circles have the same radii as the circles of ϵ_i but whose center is obtained by translating A_i by the vector $\mathbf{B_iC}$. If a point C lies in the workspace, then it must belong to the three regions ϵ_{ic} and therefore the workspace is the intersection of these three annular regions. A very simple algorithm can be used to determine these arcs. Examples are presented in Fig. 2. On a SUN 4-60 workstation the computation time for this algorithm is approx. 4–5 ms.

If the revolute joint attached to the ground cannot fully rotate, then point B_i cannot reach the full annular region ϵ_i but only an angular section of ϵ_i. From this sector a similar sector can be determined for C and the workspace is obtained as the intersection of the three angular sectors.

3. MAXIMAL WORKSPACE

The *maximal workspace* is defined as the region which the reference point C can reach with at least one orientation. It shall be noted that the maximal workspace will depend upon the choice of the reference point.

The determination of the maximal workspace has been addressed by Kassner [9] who pointed out that the boundary of this workspace is composed of circular arcs and of portions of sextic curves. However, he was only able to compute them with a discretization method. The same observation was made by Kumar [10] but was not used in the principle of the workspace computation. Indeed Kumar uses necessary conditions on the screw motion for a point to be on the boundary of the workspace, but this method cannot be used for a manipulator with prismatic actuators.

One of the objectives of the present work is to determine geometrically the boundary of the maximal workspace.

3.1. Determining if a point is in the maximal workspace

First, a simple algorithm is derived to determine if a location of the reference point is in the maximal workspace, this being equivalent to determining if there is at least one possible orientation of the platform for this location.

For a given position of C, point B_1 can move on a circle C^1_B with center C and radius $\|\mathbf{CB_1}\|$. We first verify if C^1_B is completely inside or outside the annular region ϵ_1, corresponding to the constraint for leg 1, by checking the distance between the center of C^1_B and ϵ_1 with respect to their

radii. If C_B^1 is inside ϵ_1, then any orientation is allowed for the platform, with respect to the constraints on leg 1. If C_B^1 is outside ϵ_1 then no orientation is allowed for the platform and C is outside the maximal workspace.

If the preceding test fails it may be assumed that there are intersection points between C_B^1 and ϵ_1^e, ϵ_1^i. For each of these intersection points there is a unique orientation angle possible for the platform. These angles are ordered in the interval $[0, 2\pi]$ in order to obtain a set of consecutive intervals. Then, in order to determine which intervals define valid orientations for the platform, the middle value of each interval is used as the orientation of the platform and the constraints on leg 1 are tested for the corresponding configuration. A similar procedure is performed for the legs 2 and 3. For leg i, various intervals are obtained and the set I_n^i of possible orientations of the platform with respect to the constraint on the leg can be determined (Fig. 3). The intersection $I_\cap$ of these lists is then determined by computing the intersection of all the sets of three intervals $\{I_1 \in I_n^1, I_2 \in I_n^2, I_3 \in I_n^3\}$. If $I_\cap$ is not empty then C belongs to the maximal workspace and furthermore $I_\cap$ defines the possible orientation for the moving platform at this point.

3.2. Determination of the boundary of the maximal workspace

For purposes of simplification, it is first assumed that the reference point on the platform is chosen as one of the B_is, for example point B_3. The general case will be presented later on as a generalization of the present discussion. If a location of B_3 belongs to the boundary of the maximal workspace then at least one of the legs is at an extreme value. Indeed, assuming that B_3 is on the boundary without satisfying this condition would mean that B_3 is capable of moving in any direction which is in contradiction with B_3 being on the boundary of the workspace. Note that the configuration with three legs in an extreme extension may define only isolated points of the boundary since they are solutions of the direct kinematics of the manipulator, a problem which admits at most six different solutions [11].

3.2.1. Boundary points with one extreme leg length. In order to geometrically determine the points of the boundary for which one leg length of the manipulator is at an extreme value, the kinematic chain $A_iB_iB_3$ is considered as a planar serial two-degree-of-freedom manipulator whose joint at A_i is fixed to the ground. It is well known that this manipulator is in a singular configuration when the joint centers A_i, B_i, B_3 are aligned. Consequently, the positions of B_3 belonging to the boundary of the workspace are such that A_i, B_i, B_3 lie on the same line.

For instance, consider leg 1: two types of alignment are possible. Either $A_1B_1B_3$ or $A_1B_3B_1$ (or $B_3A_1B_1$) are aligned in this order as shown in Fig. 4. Consequently, point B_3 lies on a circle C_{B_3} centered at A_i. As B_3 moves on C_{B_3}, points B_1, B_2 will move on circles denoted C_{B_1}, C_{B_2}. Valid positions of B_3 on this circle are such that the corresponding positions of B_1, B_2, B_3, respectively, belong to the annular regions ϵ_1, ϵ_2, ϵ_3 (Figs 5, 6).

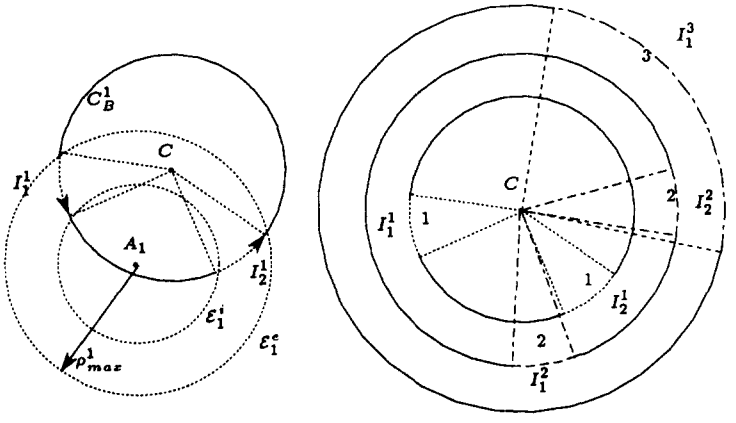

Fig. 3. For a given position of C the regions which can be reached by the B_is define three lists $\{I_i^1\}$, $\{I_m^2\}$, $\{I_n^3\}$ of intervals for the orientation of the moving platform. If C is in the maximal workspace the intersection of these lists must be non-empty. On the left is shown how the intervals $\{I_i^1\}$, $\{I_2^1\}$ are obtained. On the right it may be seen that the intersection is empty as there is no intersection between $\{I_i^1\}$ and $\{I_m^2\}$.

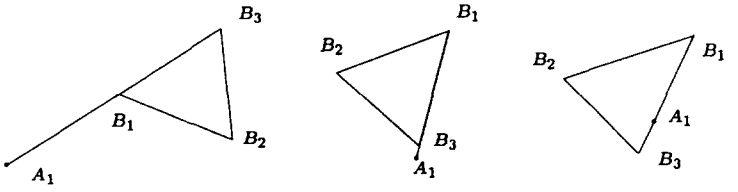

Fig. 4. If a point on the boundary is such that a leg i has an extreme extension then the points A_i, B_i, B_3 are aligned.

Let α denote the rotation angle of leg 1 around A_1. The intersection points of circle C_{B_i} with the annular region ϵ_i are then computed. All the intersection points define specific values for the angle α and the orientation of the platform. These values are ordered in a list leading to a set of intervals I^i. It is then possible to determine which intervals are components of the boundary of the workspace by taking the middle point of the arc and verifying if the corresponding pose of the platform belongs to the workspace.

As mentioned in the previous section various types of alignment are possible and some of them will lead to a component of the boundary, i.e. the motion of the platform along some direction will be forbidden. The possible cases are:

1. leg 1 in maximal extension, points $A_1B_1B_3$ aligned in this order.
2. leg 2 in maximal extension, points $A_2B_2B_3$ aligned in this order.
3. leg 1 in minimal extension, points $B_3A_1B_1$ aligned in this order.
4. leg 2 in minimal extension, points $B_3A_2B_2$ aligned in this order.
5. leg 1 in minimal extension, points $A_1B_3B_1$ aligned in this order.
6. leg 2 in minimal extension, points $A_2B_3B_2$ aligned in this order.
7. leg 1 in maximal extension, points $B_3A_1B_1$ aligned in this order.
8. leg 2 in maximal extension, points $B_3A_2B_2$ aligned in this order.

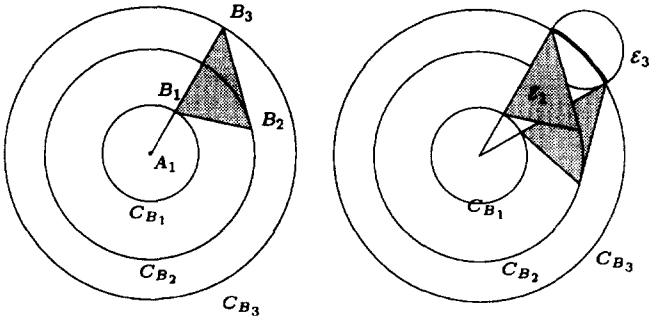

Fig. 5. When points A_1, B_1, B_3 are aligned, points B_1, B_2, B_3 lie on the circles C_{B_1}, C_{B_2}, C_{B_3} (left). The arcs on the circle C_{B_3} such that all the B_i belongs to the annular regions ϵ_i can be components of the maximal workspace boundary. On the right the valid components with respect to ϵ_3 (in thick line).

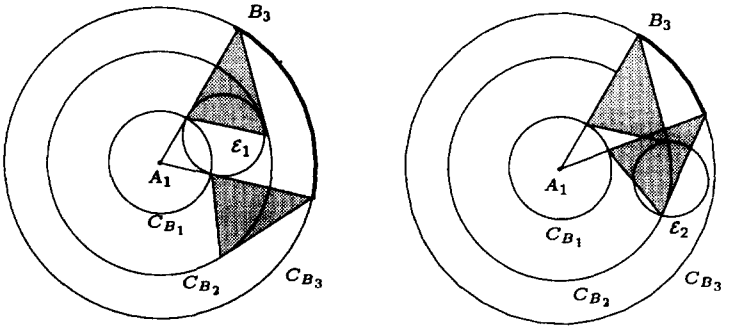

Fig. 6. On the left the valid component with respect to ϵ_1 and on the right the valid component with respect to ϵ_2 (in thick line).

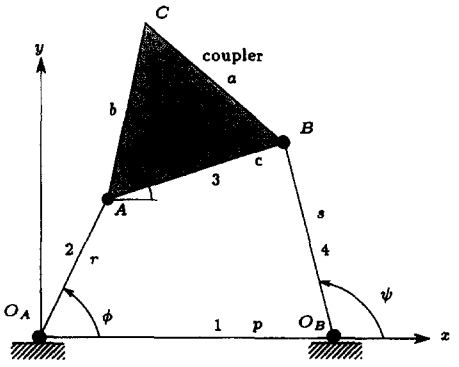

Fig. 7. The four-bar mechanism.

This arcs which are obtained after studying these different cases are placed in an appropriate structure and will be denoted *phase* 1 *arcs*.

*3.2.2. Boundary points with two extreme leg lengths.*The case for which the reference point lies on the boundary of the workspace while two leg lengths of the manipulator are in an extreme extension is now investigated. Since the reference point is point B_3, only the cases where the legs with extreme lengths are legs 1 and 2 needs to be considered.

When legs 1 and 2 have a fixed length, the trajectory of point B_3 is the coupler curve of a four-bar mechanism (Fig. 7). This mechanism has been well studied [12–14] and it is well known that the coupler curve is a sextic. Consequently it can be deduced that the boundary of the maximal workspace will be constituted of circular arcs and of portions of sextics.

Four sextics will play an important role in this study. They are the coupler curves of the four-bar mechanisms with lengths (r, s) (Fig. 7) corresponding to the various combinations of extreme lengths for legs 1 and 2, i.e. $(\rho^1_{\max}, \rho^2_{\max})$, $(\rho^1_{\max}, \rho^2_{\min})$, $(\rho^1_{\min}, \rho^2_{\min})$, $(\rho^1_{\min}, \rho^2_{\max})$.

Some particular points, referred to as the *critical points* will determine the circular arcs and the portions of sextic which define the boundary of the maximal workspace. The critical points can be of five different types, thereby defining five sets of such points.

The first set consists of the intersection points of the sextics and the annular region ϵ_3: in this case the three leg lengths are at an extreme value. Therefore, knowing these extreme values, these points are solutions of the *direct kinematics* problem [15]. This problem can be solved numerically and is known to lead to at most six solutions [11].

The second set of critical points consists of the intersection points of the sextics with the phase 1 arcs. In this case the length of legs 1 and 2 are defined by the sextics and the length of leg 3 is the radius of the arc. Consequently, these points can also be obtained from the solution of the direct kinematic problem. This problem is solved and the points which belong to the arcs are retained. These points will also be critical points for the arcs.

A third set of critical points are the multiple points of the sextics. Indeed we may have only one critical point on a circuit on the sextic: therefore introducing the multiple points as critical points enables to define two arcs of sextic on the circuit, one of them being a member of the boundary of the workspace. Finding these multiple points is a well known problem (see, for instance, [14]). In general, there are at most four double points and no triple points.

The fourth set of critical points for the sextics will be the limit points of the coupler curve. Indeed, for some value of the leg lengths the four-bar mechanism may not be a crank, i.e. the angle ϕ is restricted to belong to some intervals. Consequently the sextic is not continuous and each position of B_3 corresponding to one of the bounds of the intervals is a critical point.

The last set of critical points for the sextics consists of the set of intersection points between the sextics. Determining the intersection of two coupler curves is a difficult problem. Recently Innocenti has proposed an algorithm to solve this problem [16]. It can be shown that in the general case there will be at most 18 real intersection points and in Innocenti's method these points are obtained by solving an 18th degree polynomial. However, it is pointed out that, in the present case, the coupler curves are obtained for four-bar mechanisms which differ only by the lengths r, s. In this particular case it can be shown that there will be at most 12 real intersection points. A 12th order polynomial

was obtained for computing all the intersection points of two such sextics but this algorithm was difficult to implement and time consuming. Therefore, a simpler and faster numerical algorithm has been used here. Each sextic is divided into small components (typically 20–40) whose bounding box is easily computed and each component of the two sextics whose bounding boxes have an intersection is considered. Then, a Newton scheme is used to determine if the two components have an intersection, one of the intersection points of the bounding boxes being used as an initial guess for the solution.

3.2.3. Determination of the portions of sextic belonging to the boundary. Any portion of sextic belonging to the boundary must lie between two critical points. For each critical point T_i the unique pair of angles ϕ_i, ψ_i corresponding to T_i is determined (note that for the critical points which are multiple points of the coupler curve although the coupler point is identical the angles ϕ_i, ψ_i are different). For a given value of ϕ, there are in general two possible solutions for ψ which are obtained by solving a second order equation in the tangent of the half-angle of ψ:

$$a \tan^2\left(\frac{\psi}{2}\right) + b \tan\left(\frac{\psi}{2}\right) + c = 0$$

Consequently ψ is determined using one of the expression of the tangent of the half-angle:

$$\tan\left(\frac{\psi}{2}\right) = \frac{-b + \sqrt{b^2 - 4ac}}{2a} \quad \tan\left(\frac{\psi}{2}\right) = \frac{-b - \sqrt{b^2 - 4ac}}{2a}$$

First, the T_is are sorted according to the expression which is used for determining the corresponding angle ψ_i, thereby giving rise to two sets of T_is. Each of these sets is then sorted according to an increasing value of the angle ϕ. Consequently, the sextics are split into *arcs* of sextics, some of which are components of the boundary of the maximal workspace (Fig. 8). A component of the boundary will be such that for any point on the arc a motion along one of the normals to the sextic will lead to a violation of the constraints while a motion along the other normal will lead to feasible values for the link lengths. Any other combination implies that the arc is not a component of the boundary of the maximal workspace. In order to perform this test, the inverse Jacobian matrix for a point on the arc (for example the middle point, i.e. the coupler point obtained for ψ as the middle value between the angles ψ of the extreme points of the arc) is computed as well as the unit normal vectors $\mathbf{n}_1$, $\mathbf{n}_2$ of the sextic at this point. Then the joint velocities are calculated for a cartesian velocity directed along $\mathbf{n}_1$, $\mathbf{n}_2$. The sign of the joint velocities obtained indicates whether or not the arc is a component of the boundary. For instance, for a sextic corresponding to a maximal value of the lengths of links 1 and 2, if the joint velocities $\dot{\rho}_1$, $\dot{\rho}_2$ are both positive for a cartesian velocity along $\mathbf{n}_1$ and both negative for a cartesian velocity along $\mathbf{n}_2$, then this arc of sextic is part of the boundary. A procedure similar to the one used for the arcs of sextic is used

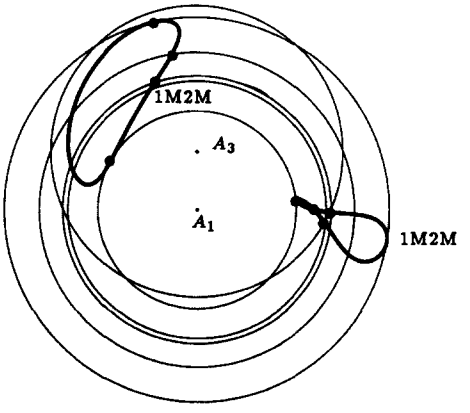

Fig. 8. Point B_3 lies on a sextic when two leg lengths are at an extreme value. This sextic (in thick lines) is split into arcs between critical points. Some of these arcs will be a component of the boundary of the maximal workspace.

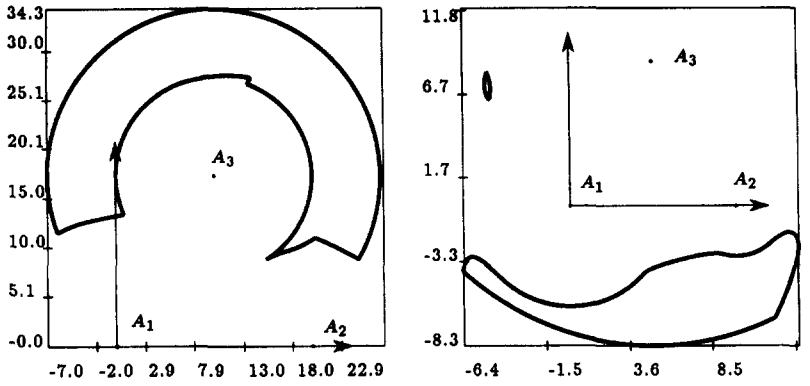

Fig. 9. On the left: the maximal workspace for manipulator 3 with $\rho_1 \in [8, 12]$, $\rho_2 \in [5, 15]$, $\rho_3 \in [10, 17]$ (computation time: 14,016 ms). On the right: the maximal workspace for manipulator 4, $\rho_1 \in [8, 12]$, $\rho_2 \in [5, 15]$, $\rho_3 \in [10, 17]$ (computation time: 1983 ms).

to identify the circular arcs which are components of the boundary. To this end, the phase 1 arcs, for which the critical points—the intersection points with the sextics and the extreme points of the arcs—have been determined, are considered. Each of the arcs between two critical points is examined to determine if the arc is a component of the boundary by using the same test as for the arcs of sextic. The boundary of the maximal workspace is finally obtained as a list of circular arcs and portions of sextics.

*3.2.4. Exception.*In general, for a given value of angle ϕ of a four-bar mechanism, there exist at most two possible values for angle ψ. However, if for example $p = r$, $\phi = 0$ and $c = s$, then angle ψ can assume any value in the interval $[0, 2\pi]$. Consequently in this case the sorting algorithm presented above must use the values of angle ψ instead of angle ϕ. A similar approach is used for the other special cases where the sort algorithm cannot be based on the various values of the angle ψ.

*3.2.5. Examples.*The maximal workspace of the manipulators described in the Appendix are shown in Figs 9, 10.

*3.2.6. Reachable regions.*Any arc of circle obtained from the phase 1 arcs is necessarily either a component of the boundary or is rejected. None of them can be fully inside the maximal workspace. This is not true for the arcs of sextics and some of them will be eliminated because they are fully inside the maximal workspace.

Some of these arcs will exhibit an interesting feature. If the intervals for the orientation of the moving platform in the neighborhood of the arc are examined, it is possible that one of the intervals will vanish when crossing the arc. If the arc splits the maximal workspace into two parts and if the initial assembly of the manipulator is such that its orientation belongs to the interval which

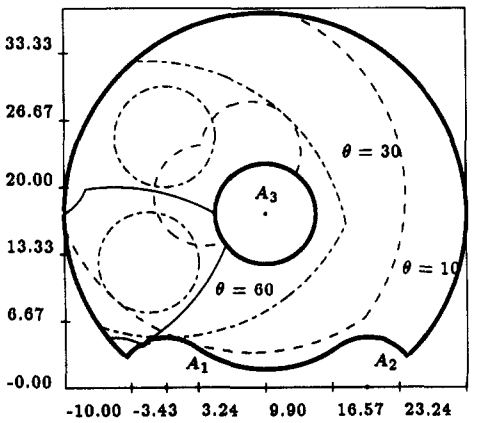

Fig. 10. The area within the thick lines is the maximal workspace of manipulator 3 with $\rho_1 \in [5, 20]$, $\rho_2 \in [5, 20]$, $\rho_3 \in [5, 20]$. The dashed and thin lines represent the constant orientation workspace for various orientations of the platform.

vanishes when crossing the arc, then the part of the workspace to which the initial assembly belongs is in fact the maximal workspace *for this initial assembly*. Any point in the other part of the workspace cannot be reached without disassembling the robot. Therefore, for each of the internal arcs of sextic whose extreme points are on the boundary of the workspace, the interval of orientation is examined by taking a random point on the arc and computing the orientation intervals for points on both sides of the arc, in the vicinity of the arc. If one of the intervals vanishes on the arc then the arc is labeled as a *separating arc* which may be a component of the maximal workspace for an initial assembly of the manipulator. Figure 11 shows an example of a separating arc.

*3.2.7. Computation time.*The computation time of the boundary of the maximal workspace is heavily dependent on the result. On a SUN 4-60 workstation this time may vary from 1500 to 15,000 ms. The most expensive part of the procedure is the calculation of the intersection of the sextics.

*3.2.8. Maximal workspace for any reference point.*In the above discussion, it was assumed that the reference point was located on point B_3. To compute the maximal workspace for any reference point, a similar algorithm can be used. Basically, only the complexity of the algorithm will be increased. Indeed, not only the eight circles of type C_1, C_2 have to be considered but also the four circles centered at A_3 which correspond to the case where the length of link 3 has an extreme value. Similarly, only the four sextics which are obtained from the extreme values of the length of links 1 and 2 have been considered in the previous section. However, the 12 sextics which can be obtained from all the possible values for the extreme lengths of links 1, 2, 3 must now be considered. Hence, all the algorithms presented above can be applied to the general case.

4. INCLUSIVE MAXIMAL WORKSPACE

The *inclusive workspace* is defined as the set of all the positions which can be reached by the reference point with at least one orientation of the platform in a given interval referred to as the *orientation interval*. This workspace will be denoted IMW. Hence, the maximal workspace is simply a particular case of IMW for which the prescribed orientation interval is $[0, 2\pi]$. In what follows, it is assumed that the orientation of the moving platform is defined by the angle between the x axis and the line B_3B_1. Moreover, it is also assumed that the reference point of the moving platform is B_3.

The computation of the boundary of the IMW is similar to the computation of the boundary of the maximal workspace. First, it is recalled that it is simple to determine if a point belongs to the IMW since one can compute the possible orientations of the moving platform at this point. It is also clear that a point lies on the boundary if and only if at least one of the link lengths is at an extreme value.

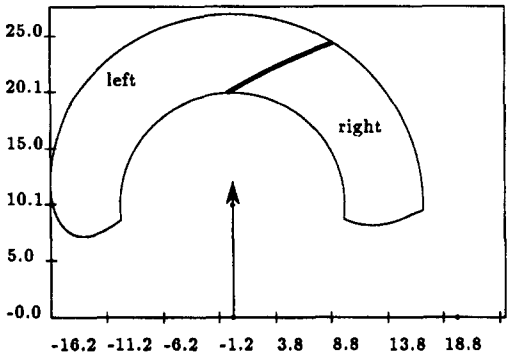

Fig. 11. The maximal workspace of a manipulator is in fact not necessarily its maximal workspace for any initial assembly. The separating arcs of the sextics allow the determination of the real maximal workspace. Here, a manipulator has been initially assembled with point B_3 positioned at (7,20) and with an orientation $\theta = 270°$. For this initial assembly, the maximal workspace is the portion of the total maximal workspace to the right of the thick line. For the initial orientation $\theta = 225°$ the maximal workspace is the total workspace (manipulator 1, $\rho_1 \in [8, 12]$, $\rho_2 \in [5, 15]$, $\rho_3 \in [10, 17]$).

Consider first the circles described by B_3 when points A_i, B_i, B_3 lie on the same line. For each position of B_3 on the circles, the orientation of the moving platform is uniquely defined. The valid circular arcs must satisfy the following constraints:

- the points B_1, B_2, B_3 lie inside the annular regions ϵ_1, ϵ_2, ϵ_3;
- the orientation of the moving platform belongs to the orientation interval.

The determination of these arcs is thus similar to obtaining the arcs when computing the maximal workspace boundary. The main difference is that building the I^j intervals involves the consideration of the rotation angle α such that the orientation of the moving platform corresponds to one of the limits of the orientation interval.

Similarly, when the sextics are considered, the positions of B_3 for which the orientation of the moving platform is at one of the limits of the orientation interval will be added in the set of critical points.

To verify if a particular arc is a component of the boundary, the orientation for a point taken at random on the arc is examined to determine if it belongs to the orientation interval. Then the test using the inverse Jacobian matrix allows to determine if the arc is a component of the boundary.

Typically the computation time for an IMW is about 1000–20,000 ms on a SUN 4-60 workstation. Figures 12, 13 present some IMW for various orientation intervals.

5. TOTAL ORIENTATION WORKSPACE

This section addresses the problem of determining the region reachable by the reference point with all the orientations in a given set $[\theta_i, \theta_j]$ which will be referred to as the orientation interval. This workspace will be denoted as TOW.

It is relatively easy to determine if a point belongs to this workspace since it is possible to compute the possible orientations for any position of the reference point. For a point belonging to the boundary of the TOW, one leg will be at an extreme value. Indeed, if a point belongs to the boundary, at least one of the legs must be at an extreme value. However, two legs cannot be at an extreme value since in that case the orientation of the moving platform is unique and consequently the point cannot belong to the TOW.

Assume that for a point on the boundary the orientation of the moving platform is one of the bounds of the interval, i.e. θ_i or θ_j while the length of leg i is at an extreme value. As B_i moves on the circle of the annular region ϵ_i corresponding to the value of the leg length, point B_3 moves on a circle C_w^i with the same radius whose center is obtained by translating the center of ϵ_i by the vector $\mathbf{B_1B_3}$, which is fixed since the orientation of the moving platform is known. Any point in the TOW must lie within the circle C_w^i. Therefore if the bounds θ_i, θ_j and all the possible B_is are considered, any point of the TOW must be inside the 12 circles with center and radii $(A_3, \rho^3_{\max})$, $(A_3, \rho^3_{\min})$, $(A_1 + \mathbf{B_1B_3}, \rho^1_{\max})$, $(A_1 + \mathbf{B_1B_3}, \rho^1_{\min})$, $(A_2 + \mathbf{B_2B_3}, \rho^2_{\max})$, $(A_2 + \mathbf{B_2B_3}, \rho^2_{\min})$.

Assume now that a point on the boundary is reached with an orientation different from θ_i, θ_j and that the length of link 1 has an extremal value, say $\rho^1_{\max}$. When the orientation of the moving platform lies in the orientation interval, B_1 belongs to an arc of circle defined by its center B_3, its radius $\|\mathbf{B_3B_1}\|$ and the angles θ_i, θ_j. As the point belongs to the TOW the arc must lie inside the annular region ϵ_1. Furthermore this arc is tangent at some point to the external circle of ϵ_1 since B_3 lies on the boundary of the TOW (Fig. 14). This tangency implies that point B_3 lies on a circle of center A_1 and radius $\rho^1_{\max} - \|\mathbf{B_1B_3}\|$. Any point within the TOW must be inside this circle. Four such circles may exist, whose center and radii are $(A_1, \rho^1_{\max} - \|\mathbf{B_1B_3}\|)$, $(A_1, \rho^1_{\min} - \|\mathbf{B_1B_3}\|)$, $(A_2, \rho^2_{\max} - \|\mathbf{B_2B_3}\|)$, $(A_2, \rho^2_{\min} - \|\mathbf{B_2B_3}\|)$.

If a point B_3 belongs to the TOW it is necessary that the point is included in the 16 circles which have been determined. Consequently the boundary of the TOW is the intersection of these 16 circles. Note that for the last four circles, theoretically, only the arcs for which the orientation of the moving platform is inside the orientation interval have to be considered. However, such arcs will be determined by the intersection of the circle with some of the initial 12 circles. The

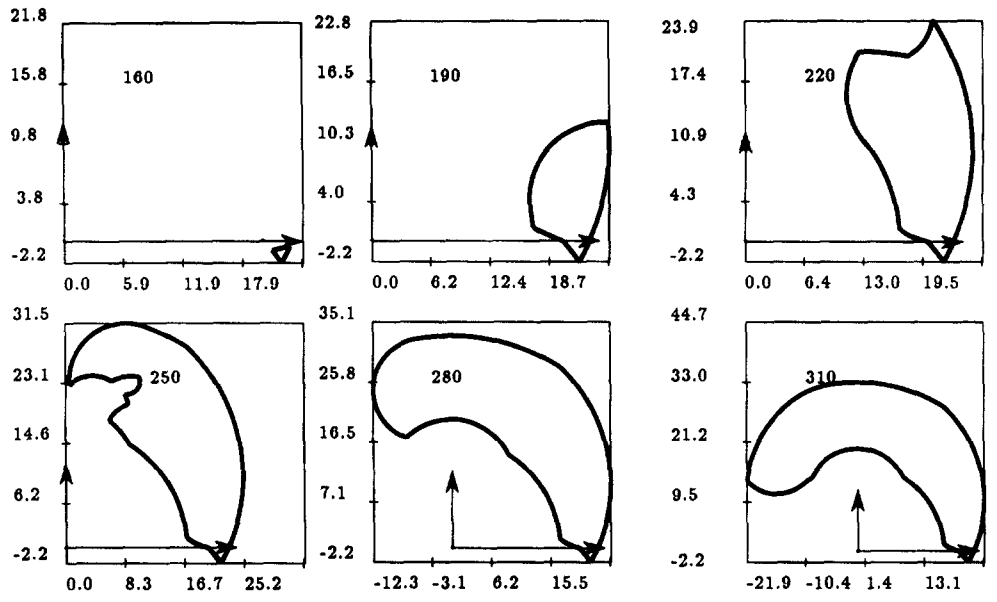

Fig. 12. IMW of manipulator 1 for various orientation intervals (the orientation intervals always begin at 0). The limits are $\rho_1 \in [2, 8]$, $\rho_2 \in [5, 25]$, $\rho_3 \in [10, 25]$.

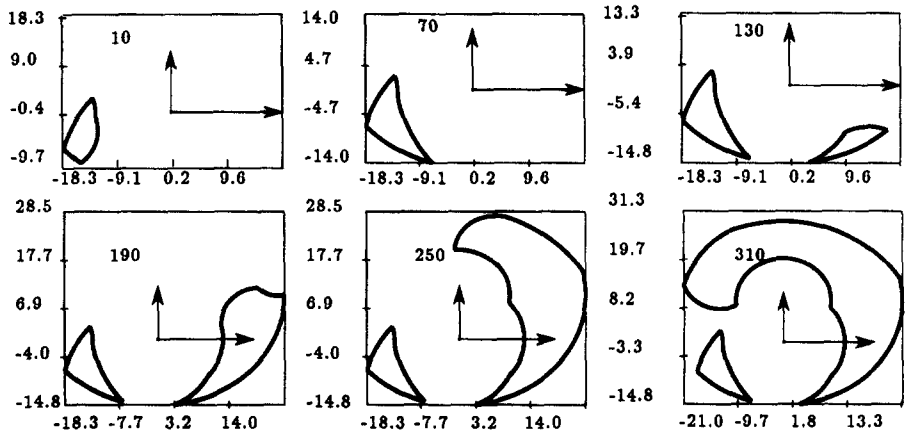

Fig. 13. IMW of manipulator 2 for various orientation intervals (the orientation intervals always begin at 0). The limits are $\rho_1 \in [2, 8]$, $\rho_2 \in [5, 25]$, $\rho_3 \in [10, 25]$.

intersection algorithm described in the section devoted to the constant orientation workspace can be used to determine the intersection of the circles.

Figures 15 and 16 illustrate some examples of TOW. The computation time is approx. 100 ms on a SUN 4-60 workstation.

6. DEXTROUS WORKSPACE

The *dextrous workspace* is the region which can be reached by the reference point with any orientation. Note that the dextrous workspace is a particular case of TOW.

Kumar [2] has used screw theory to determine the boundary of the dextrous workspace for the 3-RRR manipulator. However, his method cannot be used for manipulators with linear actuators and cannot be easily modified to take into account the mechanical limits on the joints. In [5] and [3], geometrical algorithms for the determination of the dextrous workspace of a 3-RRR manipulator have been presented. The algorithm presented in this section is similar to these algorithms.

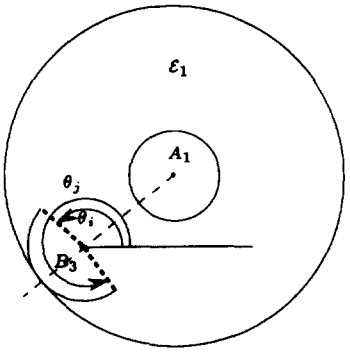

Fig. 14. Point B_3 belongs to the boundary of the TOW with the length of link 1 being ρ^1_{max}. Consequently B_1 lies on a circular arc with center B_3, radius $\|\mathbf{B_3B_1}\|$ and angles θ_i, θ_j. This arc must be included in the annular region ϵ_1 and is tangent at some point to the external circle of ϵ_1.

Let C_1 be a point belonging to the dextrous workspace. Since any orientation of the moving platform is allowed, any B_i belonging to the circle centered in C_1 with radius $\|\mathbf{CB_i}\|$ has to lie inside the annular region ϵ_i. Consequently C_1 must belong to the annular region CA_i centered in A_i whose radii are $\rho^i_{min} + \|\mathbf{CB_i}\|$ and $\rho^i_{max} - \|\mathbf{CB_i}\|$. This annular region will exist if and only if $\rho^i_{max} - \rho^i_{min} \geqslant 2\|\mathbf{CB_i}\|$ (Fig. 17, left). Therefore the dextrous workspace is the intersection of the three

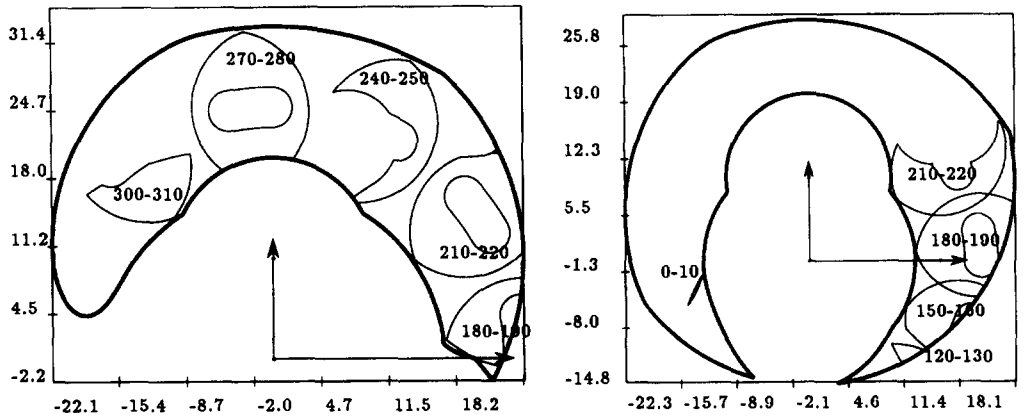

Fig. 15. Examples of total orientation workspaces for manipulators 1 and 2 with $\rho_1 \in [2, 8]$, $\rho_2 \in [5, 25]$, $\rho_3 \in [10, 25]$.

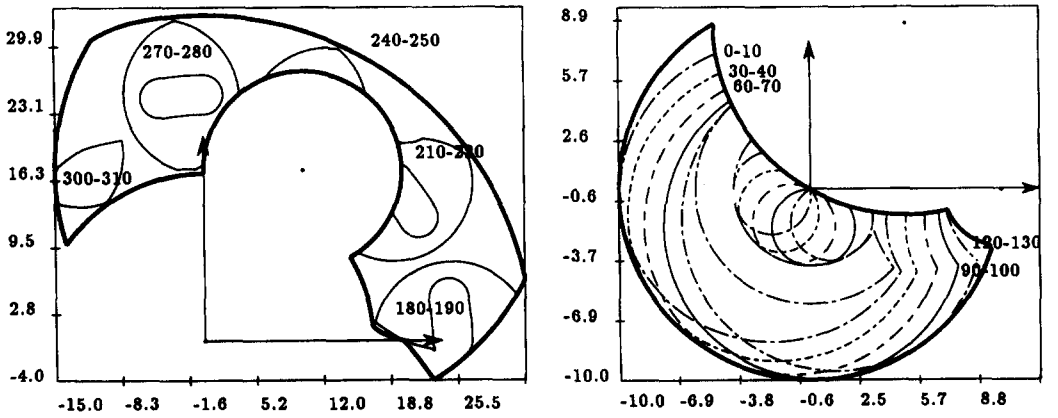

Fig. 16. Examples of total orientation workspaces for manipulators 3 and 4 with $\rho_1 \in [2, 8]$, $\rho_2 \in [5, 25]$, $\rho_3 \in [10, 25]$.

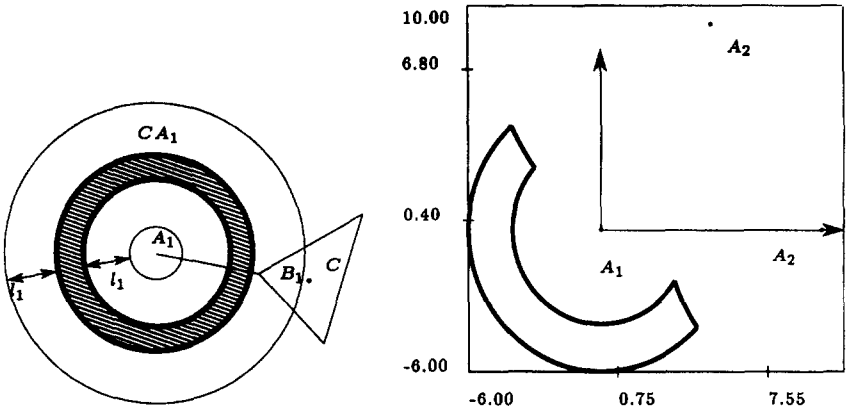

Fig. 17. On the left the dextrous workspace for C if only the constraints on link 1 are taken into account. On the right dextrous workspace for manipulator 4 ($\rho_1 \in [2, 8]$, $\rho_2 \in [5, 25]$, $\rho_3 \in [10, 25]$, computation time: 80 ms).

regions CA_i and an example is presented in Fig. 17, right. Mechanical limits on the joints can easily be included in this algorithm.

7. CONCLUSION

Geometrical algorithms for the determination of the boundary of various workspaces for planar parallel manipulators have been described. These algorithms are exact (no discretization is used) and in general their computation time is small, except for the maximal workspace.

The determination of the workspaces is very useful in the context of design or motion planning of parallel manipulators.

Acknowledgementsm—This work has been supported in part by the France–Canada collaboration contract no. 070191. *The authors wish to thank the reviewers for their useful comments.*

REFERENCES

1. Hunt, K. H., Structural kinematics of parallel actuated robot arms. *J. of Mechanisms, Transmissions and Automation in Design*, 1983, **105**, 705.
2. Kumar, V., Characterization of workspaces of parallel manipulators. *ASME J. of Mechanical Design*, 1992, **114**, 368.
3. Pennock, G. R. and Kassner, D. J., The workspace of a general geometry planar three degree of freedom platform manipulator. *ASME J. of Mechanical Design*, 1993, **115**, 269.
4. Merlet, J-P., Manipulateurs parallèles, 5eme partie: Détermination de l'espace de travail à orientation constante. Technical Report 1645, INRIA, March, 1992.
5. Williams II, R. L. and Reinholtz, C. F., Closed-form workspace determination and optimization for parallel robot mechanisms. In *ASME Proc. of the 20th Biennial Mechanisms Conf.*, Kissimmee, Orlando, 25–27 September 1988, p. 341.
6. Gosselin, C., Kinematic analysis optimization and programming of parallel robotic manipulators. Ph.D. thesis, McGill University, Montréal, 15 June 1988.
7. Ma, O. and Angeles, J., Direct kinematics and dynamics of a planar three-dof parallel manipulator. In *ASME Design and Automation Conf.*, Montréal, 17–20 September 1989, Vol. 3, p. 313.
8. Gosselin, C. and Angeles, J., The optimum kinematic design of a planar three-degree-of-freedom parallel manipulator. *J. of Mechanisms, Transmissions and Automation in Design*, 1988, **110**(1), 35.
9. Kassner, D. J., Kinematics analysis of a planar three-degree-of-freedom platform-type robot manipulator. Master's thesis, Purdue University, Purdue, December, 1990.
10. Kumar, V., Characterization of workspaces of parallel manipulators. In *ASME Proc. of the 21st Biennial Mechanisms Conf.*, Chicago, 16–19 September 1990, p. 321.
11. Gosselin, C., Sefrioui, J. and Richard, M. J., Solution polynomiale au problème de la cinématique directe des manipulateurs parallèles plans à 3 degrés de liberté. *Mechanism and Machine Theory*, 1992, **27**(2), 107.
12. Artobolevski, I., *Théorie des méanismes et des machines*. Mir, 1975.
13. Denavit, J. and Hartenberg, R. S., *Kinematic Synthesis of Linkages*. McGraw-Hill, 1964.
14. Hunt, K. H., *Kinematic Geometry of Mechanisms*. Clarendon Press, 1978.
15. Merlet, J-P., *Les Robots parallèles*. Hermès, Paris, 1990.
16. Innocenti, C., Analytical determination of the intersection of two coupler-point curves generated by two four-bar linkages. In *Computational Kinematics*, eds P. Kovacs, J. Angeles and G. Hommel. Kluwer, 1993, p. 251.

APPENDIX

The dimensions of the manipulators used in the examples of this paper are defined in Fig. A1 and their numerical values are presented in Table A1.

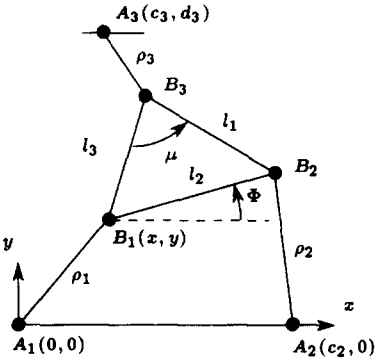

Fig. A1. Definition of the dimensions of the manipulators.

Table A1. Dimensions of the manipulators used in the examples (all the angles are in degrees). Note that μ is given since a set of l_1, l_2, l_3 leads to two possible triangles. The values of ρ_{min}, ρ_{max} are given in each example

Manipulator	Type	l_1	l_2	l_3	c_2	c_3	d_3	μ
1	RPR	25	25	25	20	0	10	60
2	RPR		20.839		17.045	16.54	15.91	0
10					52.74			
3	RPR	25	25	25	20	10	17.32	60
4	RPR	2	2	2	10	5	8.66	60